

Supplementary Information

Sulfonylation reactions photocatalyzed by quantum dots: rule of band-position and surface chemistry

Jadielson Costa,^a Danilo Galdino,^a Felipe L. N. Sousa,^b Denilson V. Freitas,^b Paula M. Jardim,^c Paulo H. Menezes^a and Marcelo Navarro^{a,*}

^a*Departamento de Química Fundamental, Universidade Federal de Pernambuco, Recife, PE, 50670-901, Brazil.*

^b*Laboratório de Pesquisa em Nanotecnologia, Centro de Tecnologias Estratégicas do Nordeste (CETENE), Recife, PE, 50740-540, Brazil*

^c*Departamento de Engenharia Metalúrgica e de Materiais – UFRJ/COPPE, Rio de Janeiro, RJ, 21941-599, Brazil.*

* *Corresponding author. Email: marcelo.navarro@ufpe.br*

Table of Contents

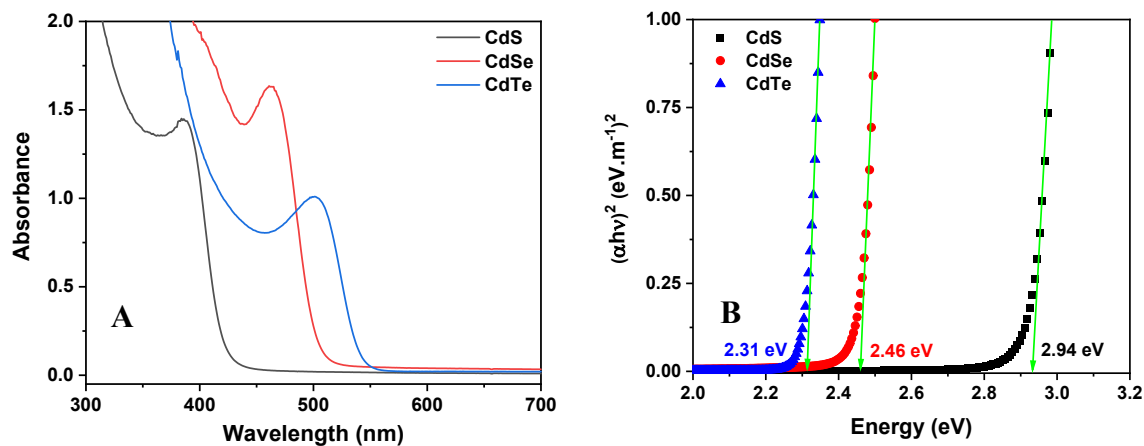
1. Chemicals	S3
2. Quantum dots	S3
2.1 Optical and Structural Characterization of the CdY QDs ($Y = S^{2-}$, Se^{2-} or Te^{2-})	S3
2.2 Cyclic Voltammetry experiments	S9
3. Photocatalyzed sulfonylation reactions	S11
3.1 Parameter optimization reactions	S11
3.2 Reaction procedures to support a radical reaction mechanism	S11
3.3 Characterization of the organic compounds	S13
3.4 1H and ^{13}C NMR Spectra of the products	S15-S26
4. EcoScale comparative analysis of sulfonylation procedures described in literature.	S27
5. References	S27

1. Chemicals

All chemicals and solvents were purchased from commercial sources and used without further purification steps. Benzyl bromide (BnBr, 99%), benzyl chloride (BnCl, 99%), and benzyl iodide (BnI, 99%), *p*-toluenesulfonic acid sodium salt (99%), benzenesulfonic acid sodium salt ($C_6H_5SO_2Na$, 99%), cysteamine (Cys, 98%), cadmium chloride ($CdCl_2$, 99.9%), 3-mercaptopropionic acid (MPA, 99%), graphite powder (99%, < 20 mesh), elemental sulphur (S, 99.98%, mesh), elemental selenium (Se, 99.5%, 100 mesh), and elemental tellurium (Te, 99.8%, 200 mesh) were purchased from Aldrich. Hydrochloric acid (HCl, 37%) was purchased from F. Maia, perchloric acid ($HClO_4$, 72%) from Merck and Ethyl acetate (98%) from Dinamica. Deionized water ($18.3 \Omega \cdot cm$) was used in cyclic voltammetry experiments.

2. Quantum dots

2.1 Optical and Structural Characterization of the CdY QDs ($Y = S^{2-}, Se^{2-}$ or Te^{2-})



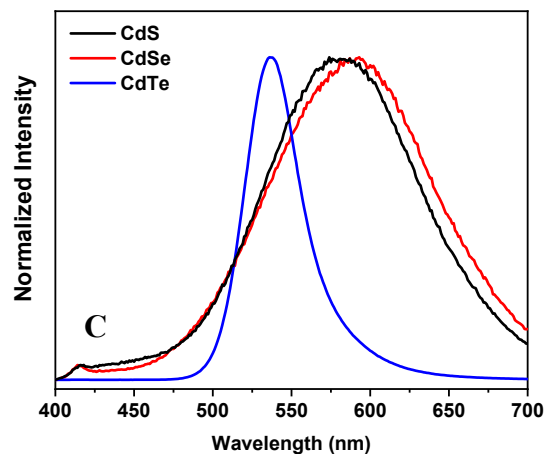


Figure S1. Optical characterization of cysteamine-capped CdS, CdSe and CdTe QDs. (A) UV-vis, (B) Tauc plot, and (C) emission spectra.

Table S1. Summary of optical properties of CdY-Cys QDs (Y = S²⁻, Se²⁻ or Te²⁻).

Sample	λ_{abs} (nm)	λ_{em} (nm)	E_g (eV)
CdS-Cys	385	578	2.94
CdTe-Cys	501	538	2.31
CdSe-Cys	463	591	2.46

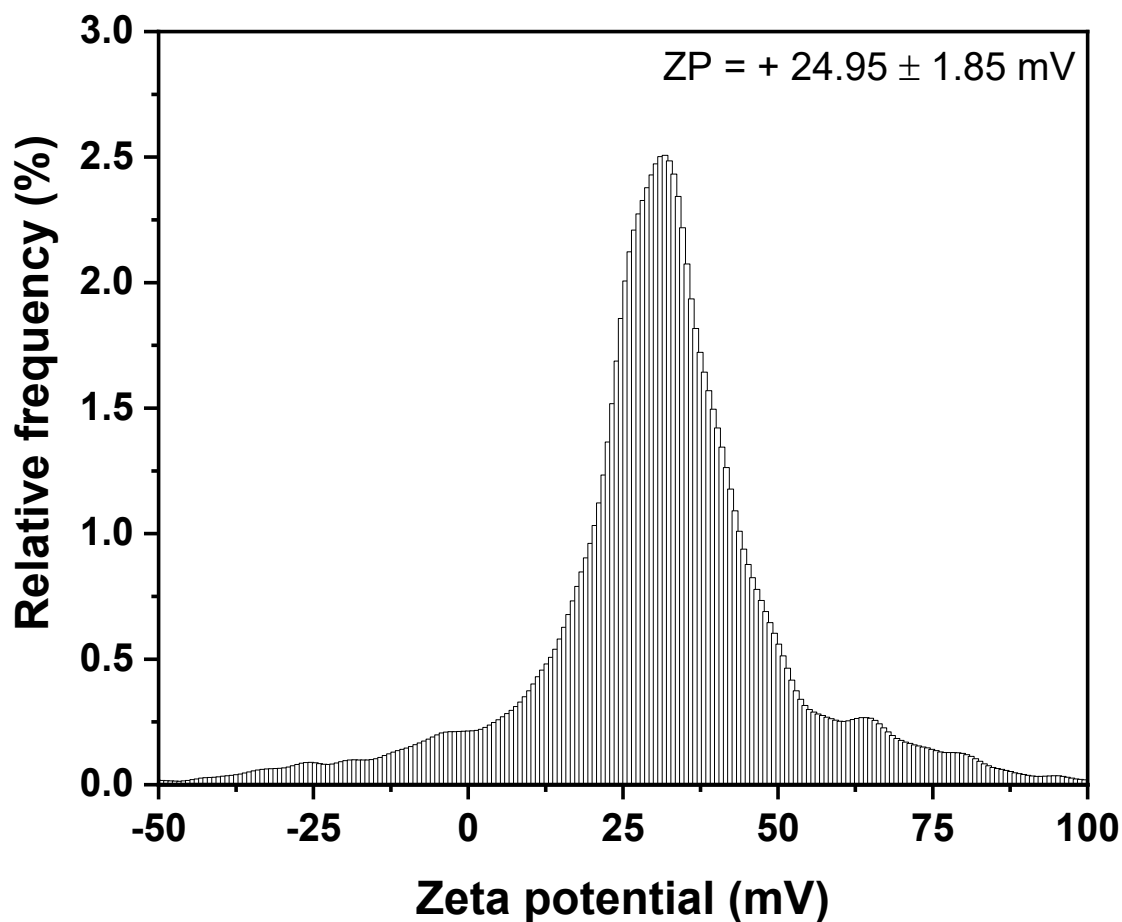


Figure S2. ZP of CdSe-Cys QDs. The interface QD/liquid plays important role for the photocatalytic performance. For CdSe-Cys, the positive surface charge was confirmed by ZP measurements (Figure S3). At pH 5.5, the cysteamine is linked to the QD surface by thiol group, and the protonated amine group interacts with aqueous solution, thus offering conditions for the QDs stabilization. The CdSe-Cys ZP value (i.e., $|\pm ZP|$) was $+ 24.95 \pm 1.85$ mV, showing a good colloidal stability.

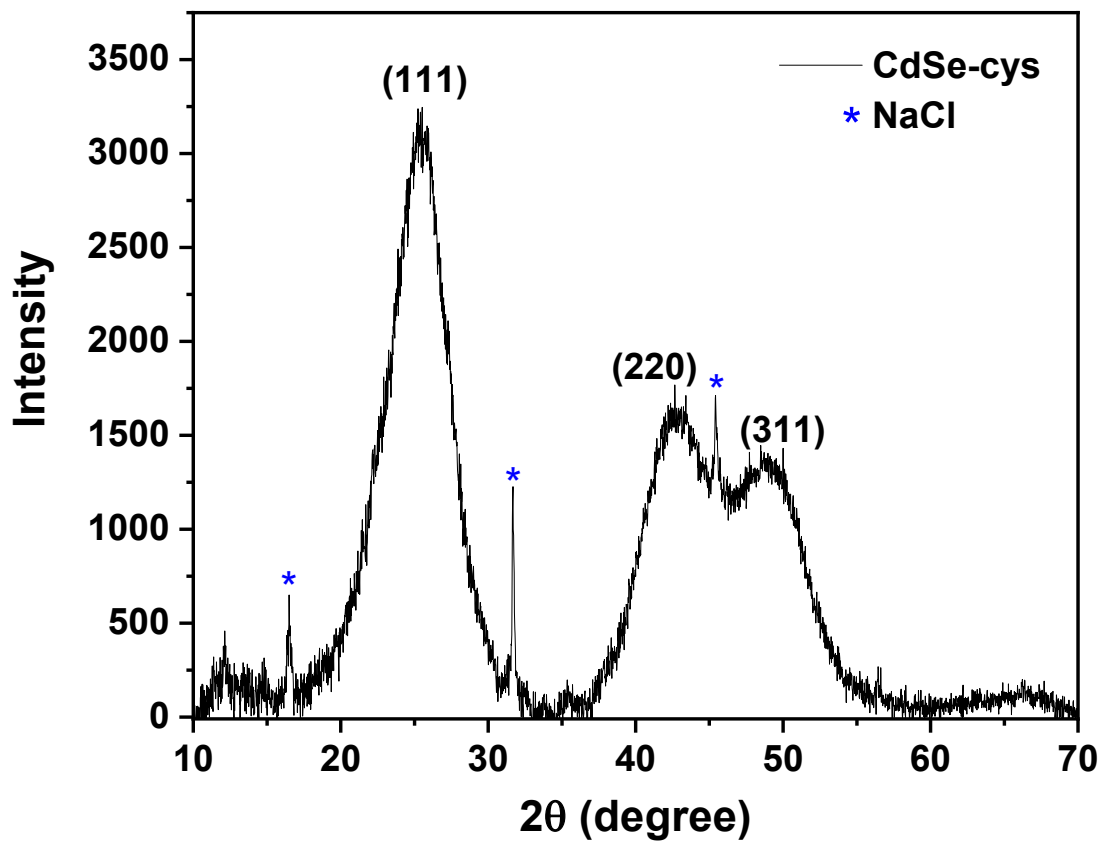


Figure S3. Powder X-ray diffractogram pattern of CdSe-Cys QDs.

Fig. S3 shows the powder X-ray diffraction patterns for the CdSe-Cys. It was observed the 2θ diffraction angles at 25.5° , 42.7° , and 48.8° , which are characteristic of planes (111), (220), and (311) of zinc blende structure pattern.

Images of solution aliquots taken during the photocatalyzed reaction, showing the CdSe-Cys DQs adsorption on the reaction product surface:

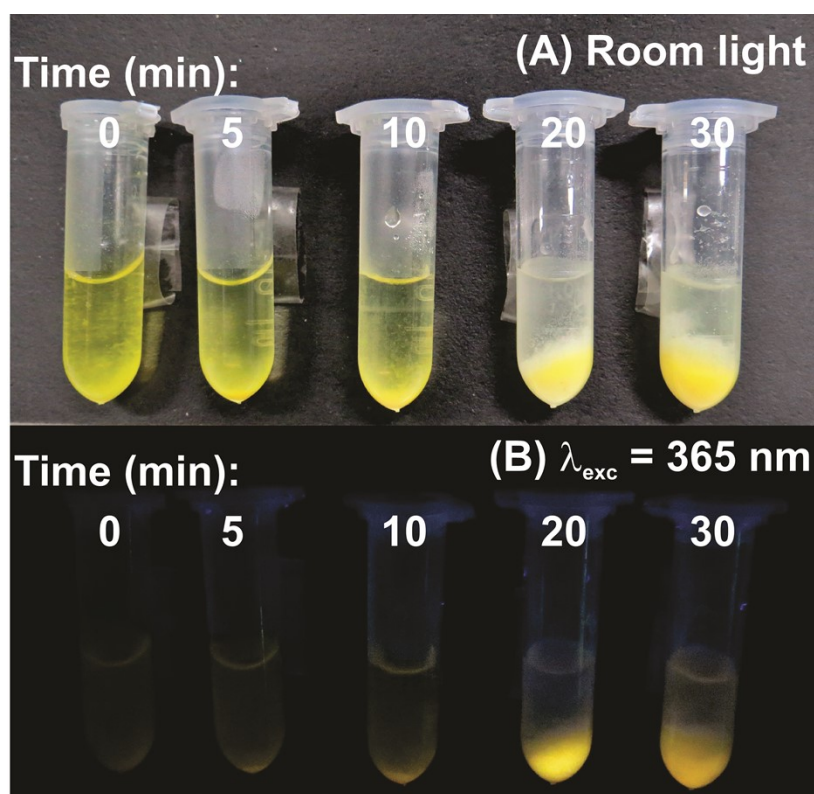


Figure S4. Reaction aliquots taken at different times ($t = 0, 5, 10, 20$ and 30 min), showing the preservation of luminescence.

The morphology and size of the quantum dots were investigated by transmission electron microscopy. The particles were diluted 1:40 in deionized water, then $5 \mu\text{L}$ of the particles were deposited on nickel transmission electron microscopy grids (100 mesh, holey carbon, SPI® Supplies), and dried overnight in a desiccator. CdSe-Cys was used as a model particle. The images were obtained in a high-resolution transmission electron microscope (HRTEM) JEOL 2100F, operating at 200 kV under different magnifications, and equipped with an energy-dispersive X-ray analyzer (EDX).

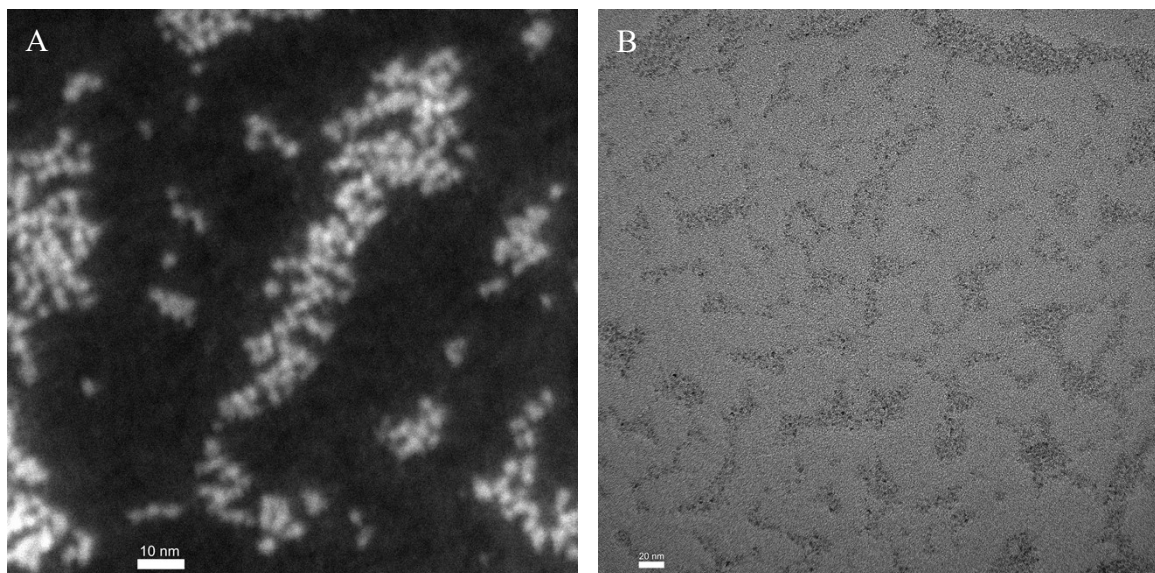


Figure S5. Morphological characterization of CdSe cysteamine capped: (A) HAADF-STEM image and (B) HRTEM image.

The image in Fig. S5A obtained by Scanning Transmission Electron Microscopy with detector of High Angle Annular Dark Field (HAADF) coupled permitted improve the contrast between the CdSe-Cys QDs and the substrate. The HRTEM image (Fig. S5B) shows the uniformity of nanoparticles distribution.

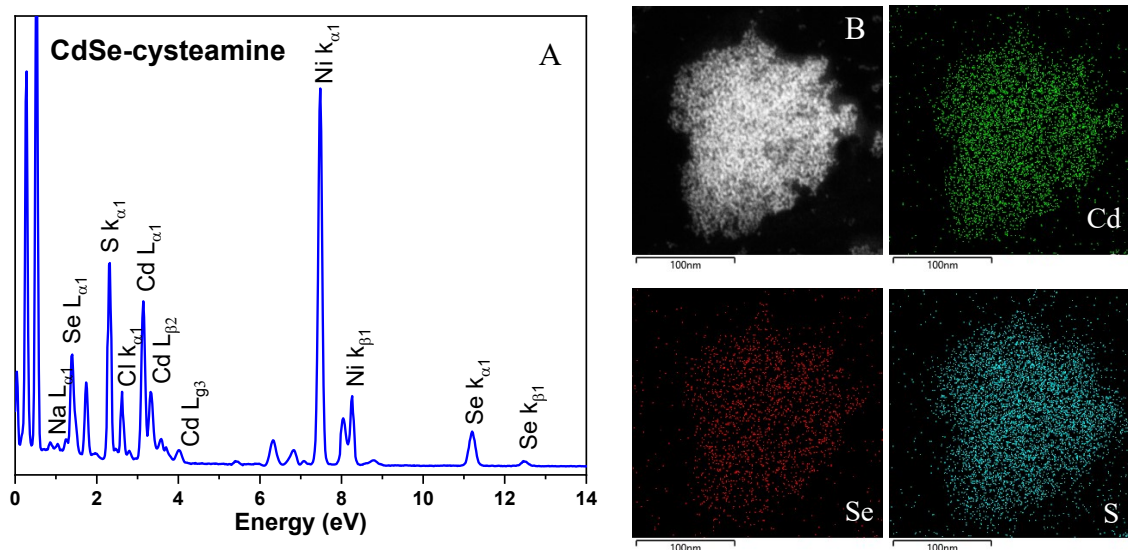


Figure S6. CdSe-Cys QDs elemental analysis: (A) EDX spectrum, and (B) Elemental mapping of cadmium (Cd), selenium (Se), and sulfur (S).

2.2 Cyclic voltammetry experiments

Cyclic voltammetry measurements were carried out at room temperature, using a Metrohm Autolab PGSTAT128N potentiostat/galvanostat and NOVA 2.0 software. Oxidation peak potential, E_{pox} , and reduction peak potential, E_{pred} , were determined by using a standard three-electrode electrochemical cell. The electrolyte was 0.01 mol.L⁻¹ Na₂SO₄ solution pH 5.5. All potential values were relative to Ag/AgCl, 3.0 mol.L⁻¹ KCl reference electrode. Vitreous carbon disk (3 mm in diameter) was used as working electrode and polished with 1 μm diamond paste; the counter electrode was a platinum wire. CV scan was started to cathodic region, from 0.0 V till -1.8 V and inverted to anodic region till 1.8 V, and stopped at 0.0 V. Scan rate was 50 mV.s⁻¹. CdSe-Cys QDs valence (E_{VB}) and conduction band (E_{CB}) energies were determined through E_{pox} and E_{pred} values by equations $E_{VB} = E_{\text{pox}} - 4.71$ eV/V and $E_{CB} = E_{\text{pred}} - 4.71$ eV/V. The electrochemical band gap energy, $E_{g\text{-electro}}$, can be associated to $\Delta E_{\text{redox}} = (E_{\text{pred}} - E_{\text{pox}})$ by using $E_{g\text{-electro}} = -\Delta E_{\text{redox}}$.^{3,4}

Cyclic voltammograms of (a) 0.01 mol.L⁻¹ Na₂SO₄ solution and (b) 1.0 mmol.L⁻¹ cysteamine in electrolyte solution (0.01 mol.L⁻¹ Na₂SO₄) are described in Figure S5.

QDs were precipitated from 25 mL of the original aqueous solutions by addition of 50 mL of acetone. The precipitation is necessary to eliminate the excess of cadmium and cysteamine present in the aqueous solution of the QDs. Thus, the acetone/water solution was centrifuged during 20 min at 5000 rpm. QDs precipitated on the walls of the recipient and the acetone/water solution was extracted, resulting in only solid QDs, which were dried under vacuum. 1 mg of the QDs was re-suspended in 1.8 mL of distilled water followed by addition of 0.2 mL of 0.1 mol.L⁻¹ Na₂SO₄ solution. Cyclic voltammograms of CdY-Cys QDs (Y = S, Se or Te) (Fig. 2 in the article) were carried out in 0.01 mol.L⁻¹ Na₂SO₄ solution.

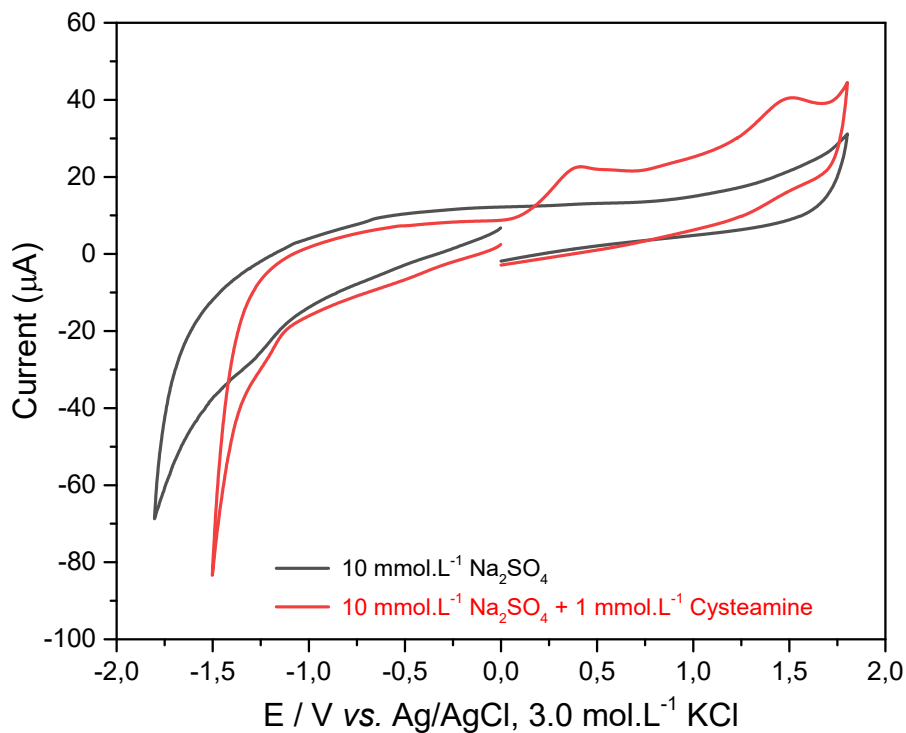


Figure S7. Cyclic voltammograms of (a) 0.01 mol.L⁻¹ Na₂SO₄ solution, (b) 1.0 mmol.L⁻¹ cysteamine. Vitreous carbon disk (3 mm in diameter) working electrode, Pt wire counter electrode and Ag/AgCl (3.0 mol.L⁻¹ KCl solution) reference electrode. Scan rate was 50 mV.s⁻¹.

3. Photocatalyzed sulfonylation reactions

Table S2 – **3a** product yields obtained from sulfonylation reactions (**1a** + **2a**) carried out in CdSe-Cys aqueous solution recovered following 1 to 5 catalytic cycles, after ethyl acetate extractions.

Entry	Catalytic cycle	Yield ^a (%)
1	1	92
2	2	92
3	3	90
4	4	87
5	5	84

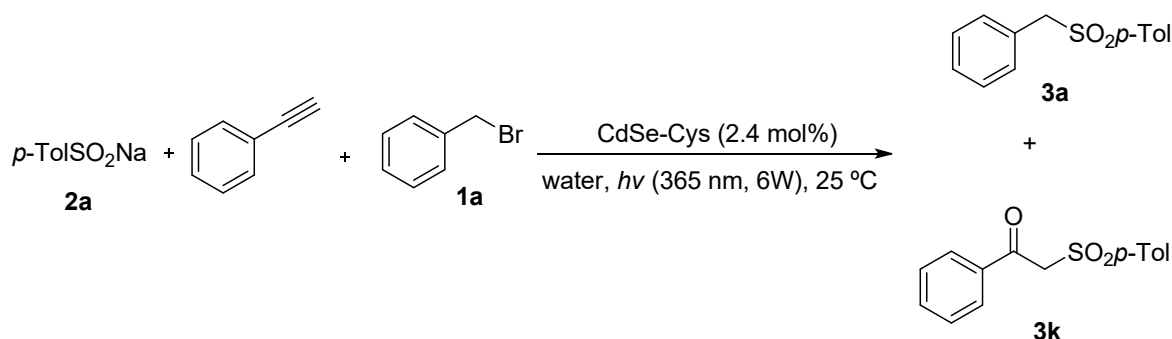
^a Isolated product.

3.1 Parameter optimization reactions

The same procedure described in 3.1 (*General Procedure for the Synthesis of Sulfones (3a-n)*) was used to carry out the optimization of parameters. Only specific parameters of the experimental conditions were modified according to Scheme 2 of the article: a) no UV light; no QDs were added to the reaction medium; or the reaction was performed under argon atmosphere, b) reaction performed in absence of **2a** reagent, c) reaction performed in absence of **1a** reagent.

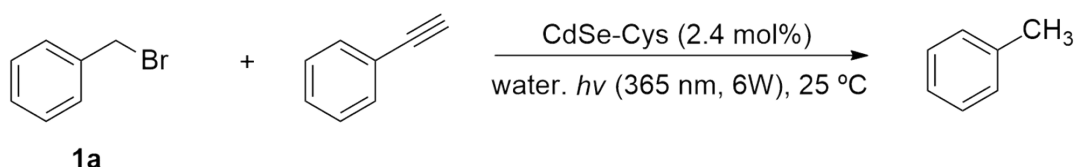
3.2 Reaction procedures to support a radical reaction mechanism

3.2.1 Photocatalyzed competition reaction between benzyl bromide, sodium *p*-toluenesulfinate and phenylacetylene



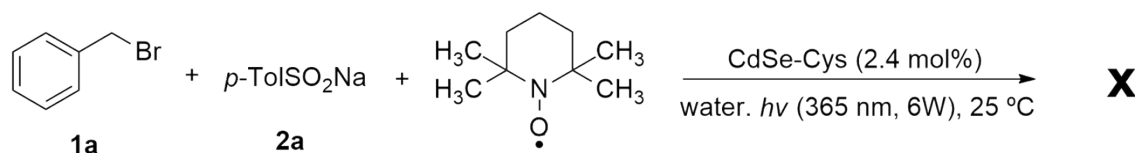
6 mL of CdSe-Cys colloidal solution was added to a 10 mL glass flask containing benzyl bromide (**1a**) (0.25 mmol), sodium *p*-toluenesulfinate **2a** (0.56 mmol) and phenylacetylene (0.25 mmol). The mixture was stirred under UV light (365 nm). After 4 hours, the mixture was diluted with 10 mL of water and extracted with ethyl acetate (3 x 10 mL) in a separatory funnel. The organic phase was dried with Na₂SO₄, filtered and rotaevaporated. The mixture was separated by column chromatography (hexane/acetate 8:2) giving **3a** (73%) and **3k** (22%) of isolated products.

3.2.2 Photocatalyzed reaction between benzyl bromide and phenylacetylene



6 mL of CdSe-Cys colloidal solution was added to a 10 mL glass flask containing benzyl bromide **1a** (0.5 mmol) and phenylacetylene (0.5 mmol). The mixture was stirred under UV light (365 nm). After 2 hours, the mixture was diluted with 10 mL of water and extracted with ethyl acetate (3 x 10 mL) in a separatory funnel. The organic phase was dried with Na₂SO₄, filtered, and analyzed by GC. 56% of toluene was determined (chromatographic yield) as the only reaction product.

3.2.3 Photocatalyzed reaction between **1a** and **2a** in the presence of TEMPO



6 mL of CdSe-Cys colloidal solution was added to a 10 mL glass flask containing **1a** (0.5 mmol), **2a** (0.56 mmol) and TEMPO (2,2,6,6-tetramethylpiperidine-N-oxyl) (0.5 mmol). The mixture was stirred under UV light (365 nm) for 2 hours. After, the mixture was diluted with 10 mL of water and extracted with ethyl acetate (3 x 10 mL) in a separatory funnel. The organic phase was dried with Na₂SO₄, filtered, and analyzed by GC. No reaction product was identified, showing the inhibitory effect of TEMPO reagent.

3.3 Characterization of the organic compounds

During photocatalysis reactions, to keep up with the product evolution and total conversion, GC/FID analysis was carried out on a Varian CP-3380 gas chromatograph system coupled with a flame ionization detector; coupled with a chromatographic column capillary column (Chrompack CP-SPL5CB, 30 m × 0.25 mm, 0.25 μm) using the initial temperature 60 °C then increased to 220 °C at rate of 10 °C.min⁻¹. Thermo Scientific model ISQ 7000 single quadrupole electronic ionization mass spectrometer coupled to the Thermo Scientific model Trace 1310 chromatograph was used for GC/MS spectra. Varian spectrometer model Unity Plus 300 MHz or Varian spectrometer model URMNS 400 MHz were used for NMR spectra. ¹H and ¹³C nuclear magnetic resonance (NMR) data were recorded in CDCl₃. The chemical shifts are reported as delta (δ) units in parts per million (ppm) relative to the solvent residual peak as the internal reference [δ 7.26 (¹H NMR) and δ 77.16 (¹³C NMR)]. Coupling constants (J) for all spectra are reported in Hertz (Hz).

1-(benzylsulfonyl)-4-methylbenzene (3a): Obtained 108 mg (88%) as a white solid. ¹H NMR (400 MHz, CDCl₃) δ 7.50 (d, *J* = 8 Hz, 2H), 7.35 – 7.20 (m, 5H), 7.09 (d, *J* = 8 Hz, 2H), 4.29 (s, 2H), 2.42 (s, 3H). ¹³C NMR (100 MHz, CDCl₃) δ 144.8, 135.1, 131.0, 129.6, 128.8, 128.8, 128.7, 128.4, 63.0, 21.8. The data match to the previously described compound.⁵

1-methyl-4-((4-nitrobenzyl)sulfonyl)benzene (3b): Obtained 166 mg (90%) as a white solid. ¹H NMR (400 MHz, CDCl₃) δ 8.14 (d, *J* = 8.8 Hz, 2H), 7.54 (d, *J* = 8.0 Hz, 2H), 7.35 – 7.28 (m, 4H), 4.39 (s, 2H), 2.45 (s, 3H). ¹³C NMR (100 MHz, CDCl₃) δ 148.2, 145.6, 135.6, 134.7, 131.9, 130.0, 128.7, 123.8, 62.4, 21.8. The data match to the previously described compound.⁵

4-(tosylmethyl)benzotrile (3c): Obtained 132 mg (98%) as a white solid. ¹H NMR (600 MHz, CDCl₃) δ 7.57 (d, *J* = 8.4 Hz, 2H), 7.51 (d, *J* = 8.4 Hz, 2H), 4.33 (s, 2H), 2.44 (s, 3H). ¹³C NMR (150 MHz, CDCl₃) δ 145.4, 132.4, 131.7, 130.0, 128.7, 62.7, 21.8. The data match to the previously described compound.⁶

1-methoxy-4-(tosylmethyl)benzene (3d): Obtained 122 mg (88%) as a white solid. ^1H NMR (400 MHz, CDCl_3) δ 7.50 (d, $J = 8$ Hz, 2H), 7.24 (d, $J = 8$ Hz, 2H), 7.00 (d, $J = 8.7$ Hz, 2H), 6.78 (d, $J = 8.7$ Hz, 2H), 4.22 (s, 2H), 3.78 (s, 3H), 2.41 (s, 3H). ^{13}C NMR (100 MHz, CDCl_3) δ 160.1, 144.7, 135.2, 132.1, 129.6, 128.8, 120.3, 114.1, 62.4, 55.4, 21.8. The data match to the previously described compound.⁵

1-(allylsulfonyl)-4-methylbenzene (3e): Obtained 96 mg (97%) as a pale yellow oil. ^1H NMR (400 MHz, CDCl_3): δ 7.70 (d, $J = 8$ Hz, 2H), 7.30 (d, $J = 8$ Hz, 2H), 5.74 (ddt, $J = 17.2, 10, 7.2$ Hz, 1H), 5.28 (d, $J = 10$ Hz, 1H), 5.11 (d, $J = 17.2$, 1H), 3.76 (d, $J = 7.2$ Hz, 2H), 2.40 (s, 3H). ^{13}C NMR (100 MHz, CDCl_3) δ 144.8, 135.3, 129.7, 128.5, 124.8, 124.6, 60.9, 21.6. The data match to the previously described compound.⁷

Ethyl 2-tosylacetate (3f): Obtained 99 mg (82%) as a pale yellow oil. ^1H NMR (400 MHz, CDCl_3) δ 7.82 (d, $J = 8.4$ Hz, 2H), 7.37 (d, $J = 8.4$ Hz, 2H), 4.18 – 4.10 (m, 4H), 2.45 (s, 3H), 1.19 (t, $J = 7.1$ Hz, 3H). ^{13}C NMR (100 MHz, CDCl_3) δ 162.5, 145.5, 135.7, 129.8, 128.5, 62.3, 61.0, 21.7, 13.8. The data match to the previously described compound.⁸

Ethyl 2-tosylpropanoate (3g): Obtained 110 mg (84%) as pale yellow oil. ^1H NMR (400 MHz, CDCl_3) δ 7.73 (d, $J = 8.4$ Hz, 2H), 7.33 (d, $J = 8.4$ Hz, 2H), 4.09 (q, $J = 7.2$ Hz, 2H), 4.00 (q, $J = 7.6$ Hz, 1H), 2.42 (s, 3H), 1.52 (d, $J = 7.6$ Hz, 3H), 1.14 (t, $J = 7.2$ Hz, 3H). ^{13}C NMR (100 MHz, CDCl_3) δ 166.4, 145.4, 134.0, 129.7, 129.4, 65.5, 62.2, 21.7, 13.9, 11.9. The data match to the previously described compound.⁹

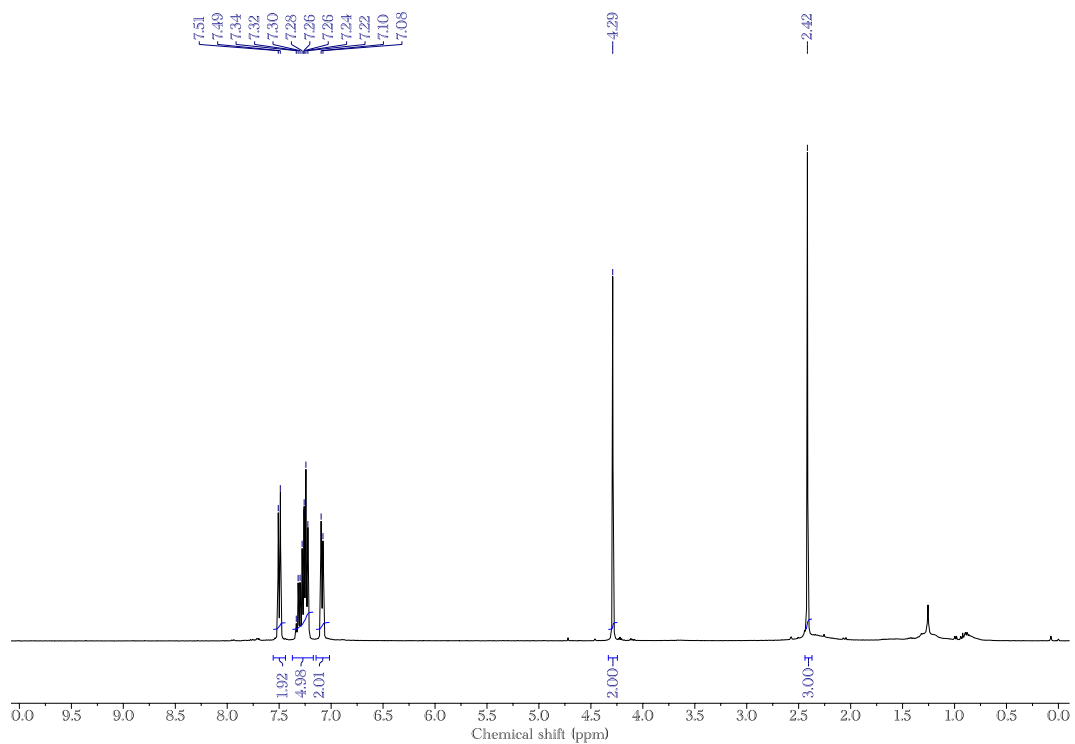
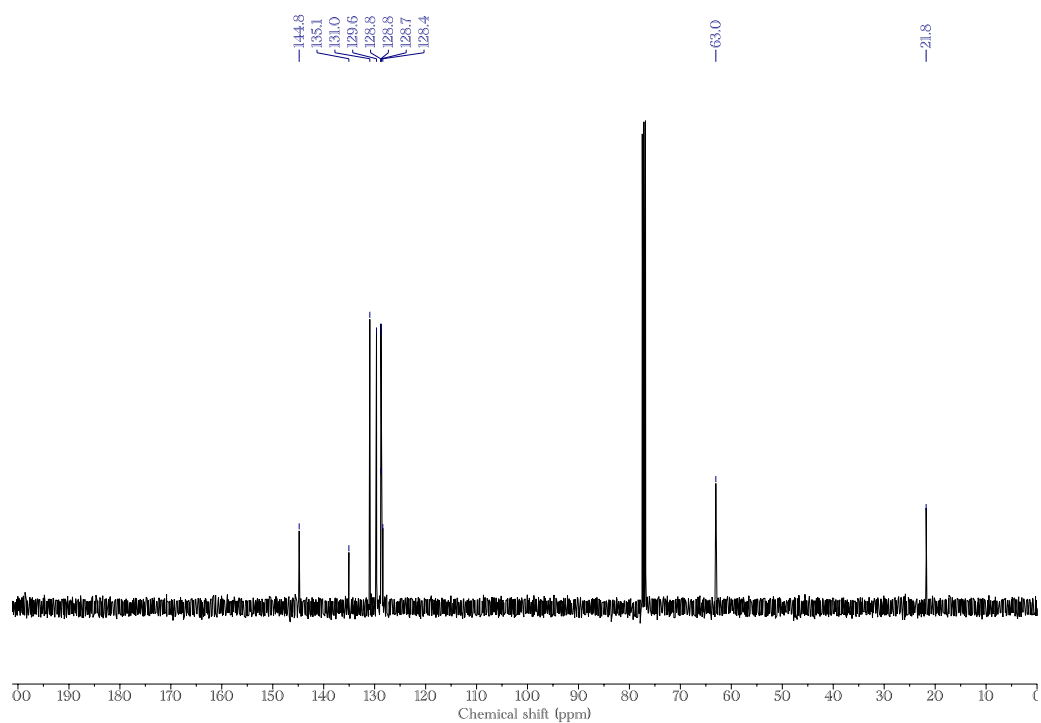
1-phenyl-2-tosylethan-1-one (3k): Obtained 117 mg (93%) as yellow solid. ^1H NMR (400 MHz, CDCl_3) δ 7.94 (d, $J = 7.2$ Hz, 2H), 7.76 (d, $J = 8.4$ Hz, 2H), 7.61 (t, $J = 7.2$ Hz, 1H), 7.47 (t, $J = 8$ Hz, 2H), 7.33 (d, $J = 8$ Hz, 2H), 4.72 (s, 2H), 2.44 (s, 3H). ^{13}C NMR (100 MHz, CDCl_3) δ 188.3, 145.5, 135.9, 134.4, 129.9, 129.4, 128.9, 128.7, 63.7, 21.8. The data match to the previously described compound.¹⁰

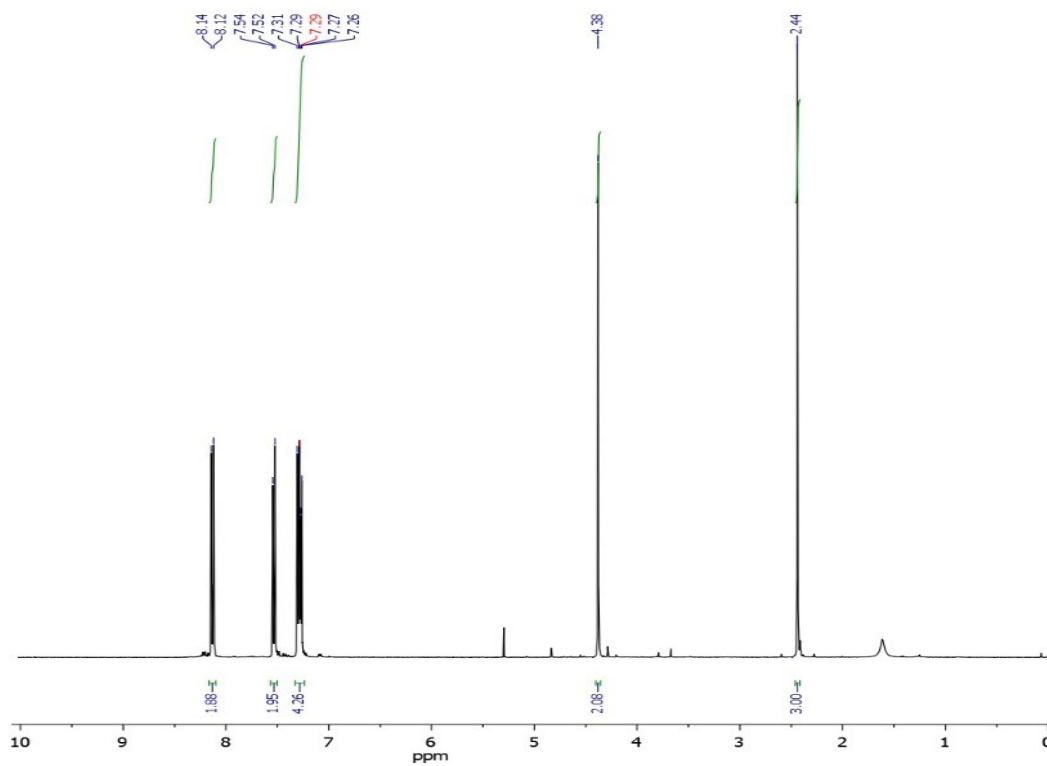
1-(4-methoxyphenyl)-2-tosylethan-1-one (3l): Obtained 126 mg (83%) as a white solid. ^1H NMR (400 MHz, CDCl_3) δ 7.91 (d, $J = 9.2$ Hz, 2H), 7.74 (d, $J = 8.4$ Hz, 2H), 7.31 (d, $J = 8.4$ Hz, 2H), 6.92 (d, $J = 9.2$ Hz, 2H), 4.67 (s, 2H), 3.85 (s, 3H), 2.42 (s, 3H). ^{13}C NMR (100

MHz, CDCl₃) δ 186.4, 164.5, 145.2, 135.9, 131.9, 129.8, 128.9, 128.5, 114.0, 63.4, 55.6, 21.7. The data match to the previously described compound.¹⁰

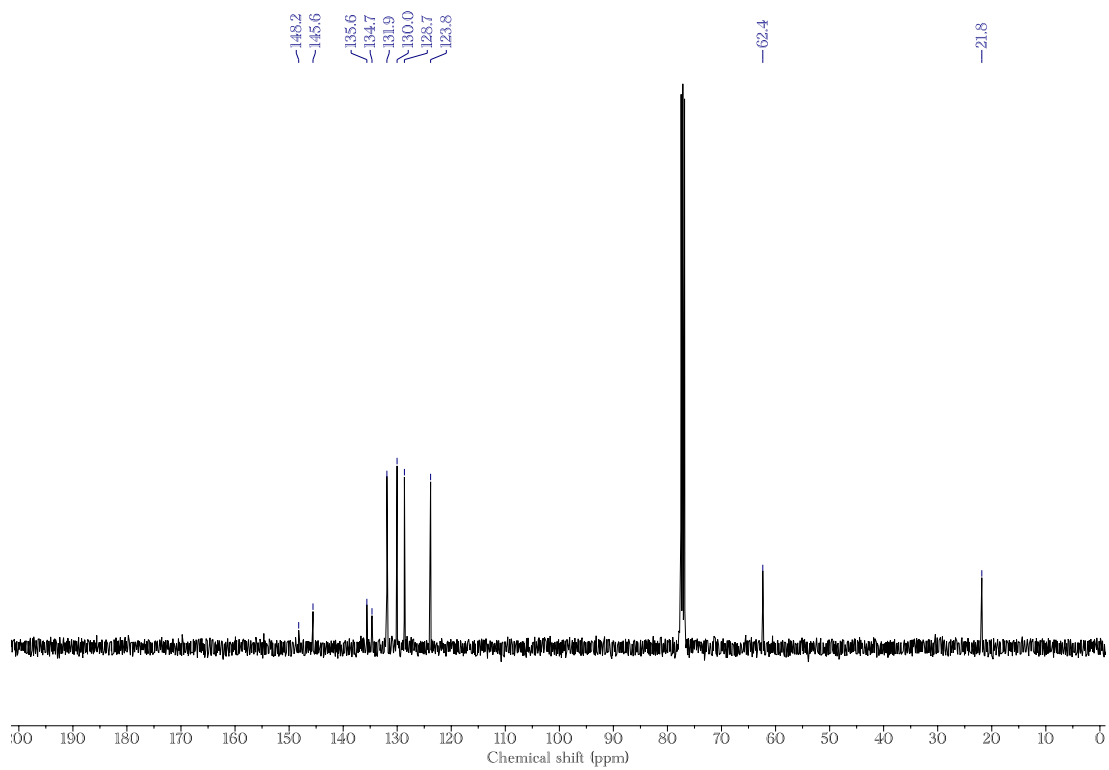
1-(4-nitrophenyl)-2-tosylethan-1-one (3m): Obtained 139 mg (87%) as a pale-yellow solid. ¹H NMR (400 MHz, CDCl₃) δ 8.31 (d, J = 9.2 Hz, 2H), 8.14 (d, J = 9.2 Hz, 2H), 7.73 (d, J = 8 Hz, 2H), 7.35 (d, J = 8 Hz, 2H), 4.76 (s, 2H), 2.45 (s, 3H). ¹³C NMR (100 MHz, CDCl₃) δ 187.2, 150.9, 146.0, 140.0, 135.4, 130.6, 130.2, 128.6, 124.1, 64.2, 21.8. The data match to the previously described compound.¹⁰

(Benzylsulfonyl)benzene (3n): Obtained 108 mg (93%) as a white solid. ¹H NMR (400 MHz, CDCl₃) δ 7.59 – 7.48 (m, 3H), 7.37 (t, J = 7.6 Hz, 2H), 7.23 (d, J = 7.2 Hz, 1H), 7.18 (t, J = 7.6 Hz, 2H), 7.01 (d, J = 7.2 Hz, 2H), 4.24 (s, 2H). ¹³C NMR (100 MHz, CDCl₃) δ 137.9, 133.8, 130.9, 129.0, 128.9, 128.8, 128.7, 128.2, 63.0. The data match to the previously described compound.¹¹

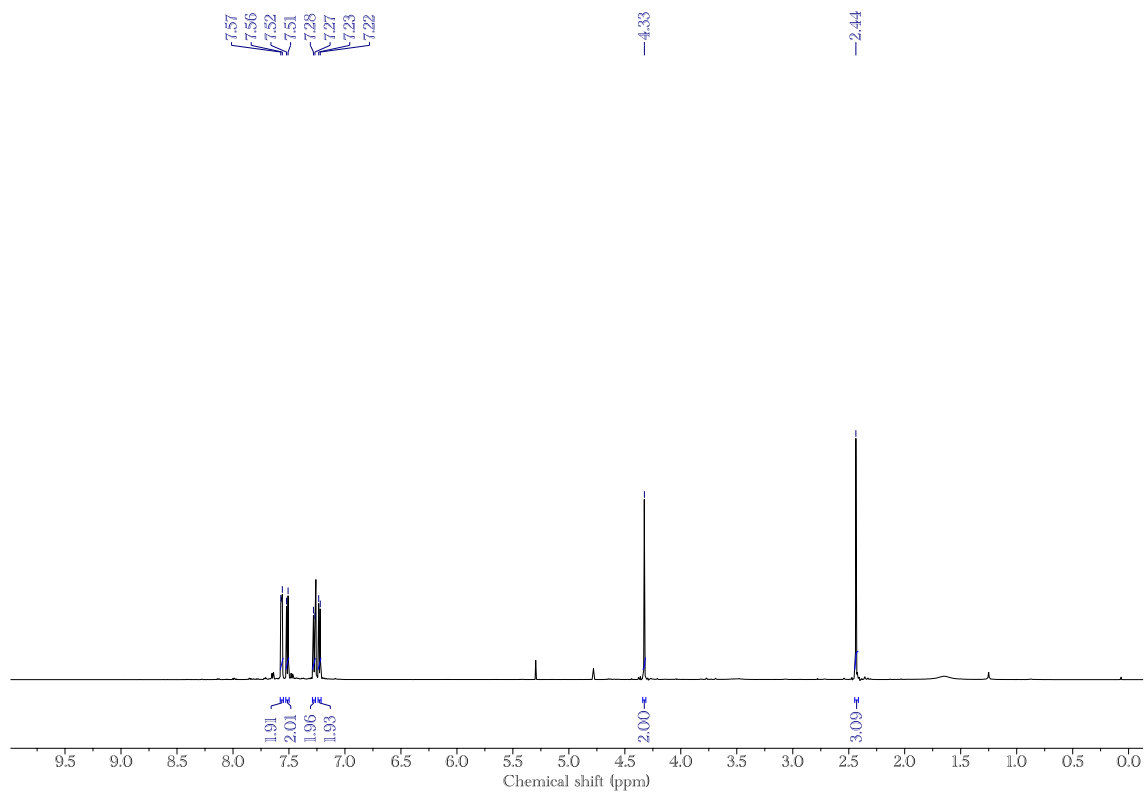
3.4 ^1H and ^{13}C NMR spectra of the products ^1H NMR spectrum (400 MHz, CDCl_3) of compound 3a ^{13}C NMR spectrum (100 MHz, CDCl_3) of compound 3a



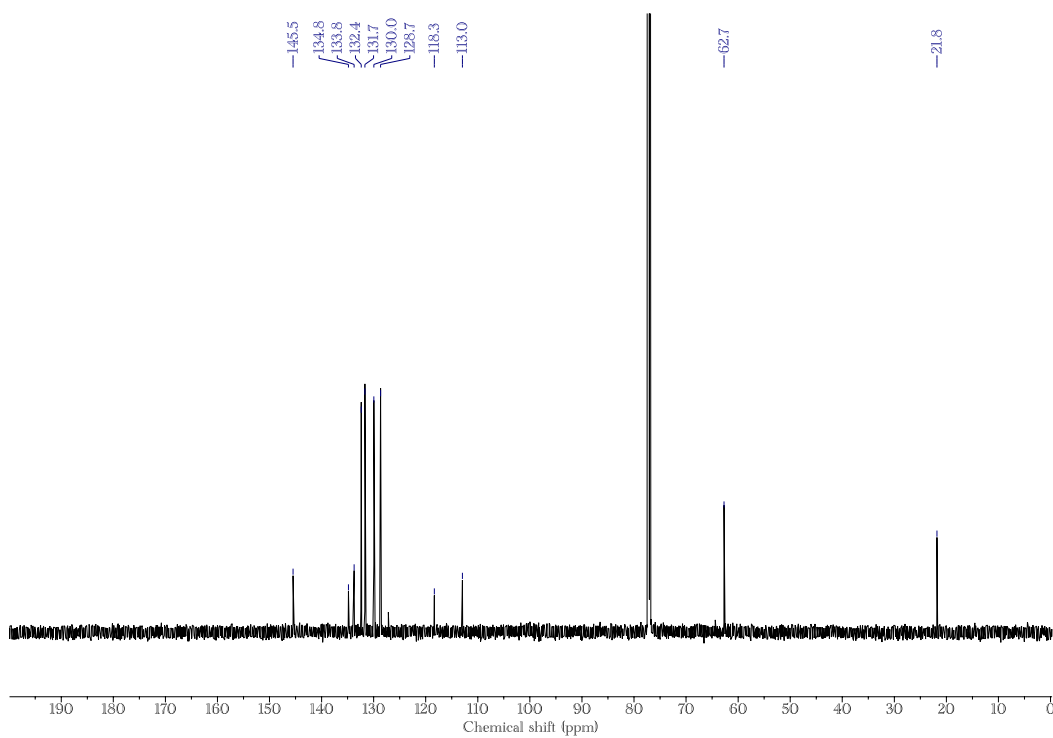
¹H NMR spectrum (400 MHz, CDCl₃) of compound 3b



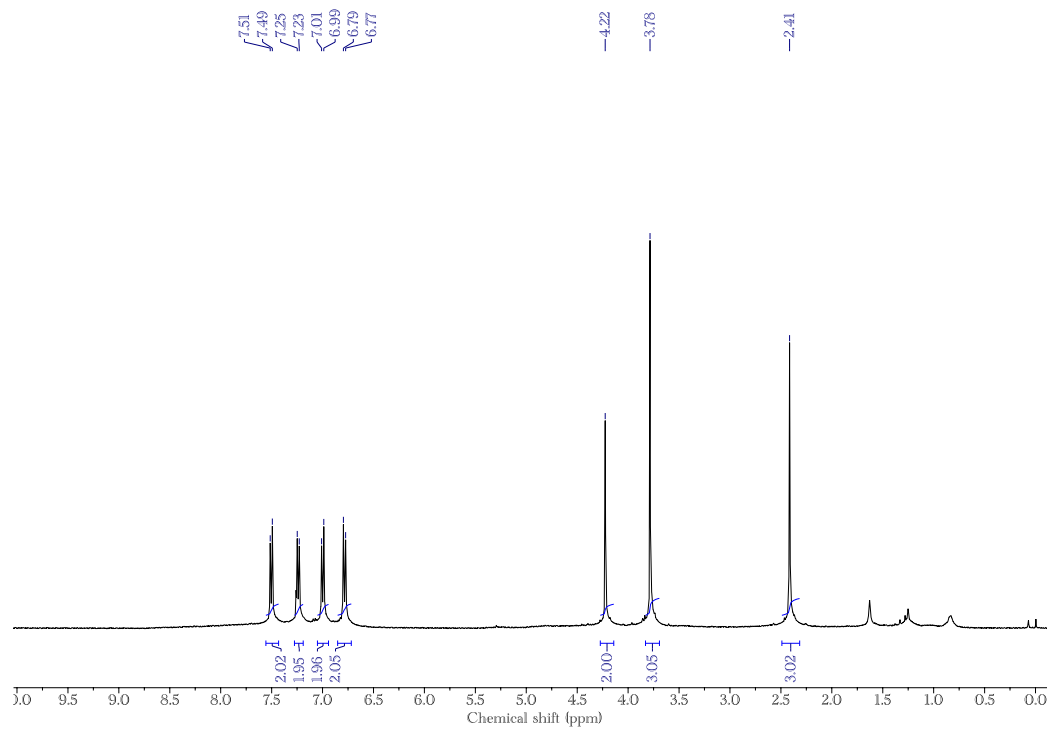
¹³C NMR spectrum (100 MHz, CDCl₃) of compound 3b



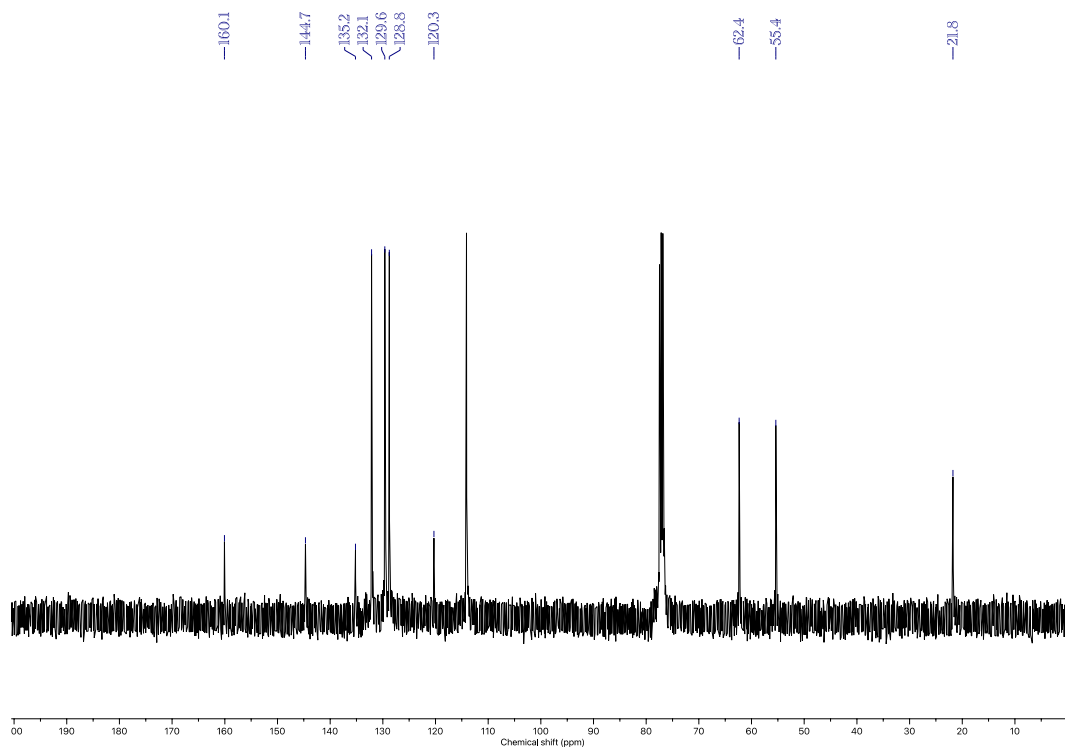
¹H NMR spectrum (600 MHz, CDCl₃) of compound 3c



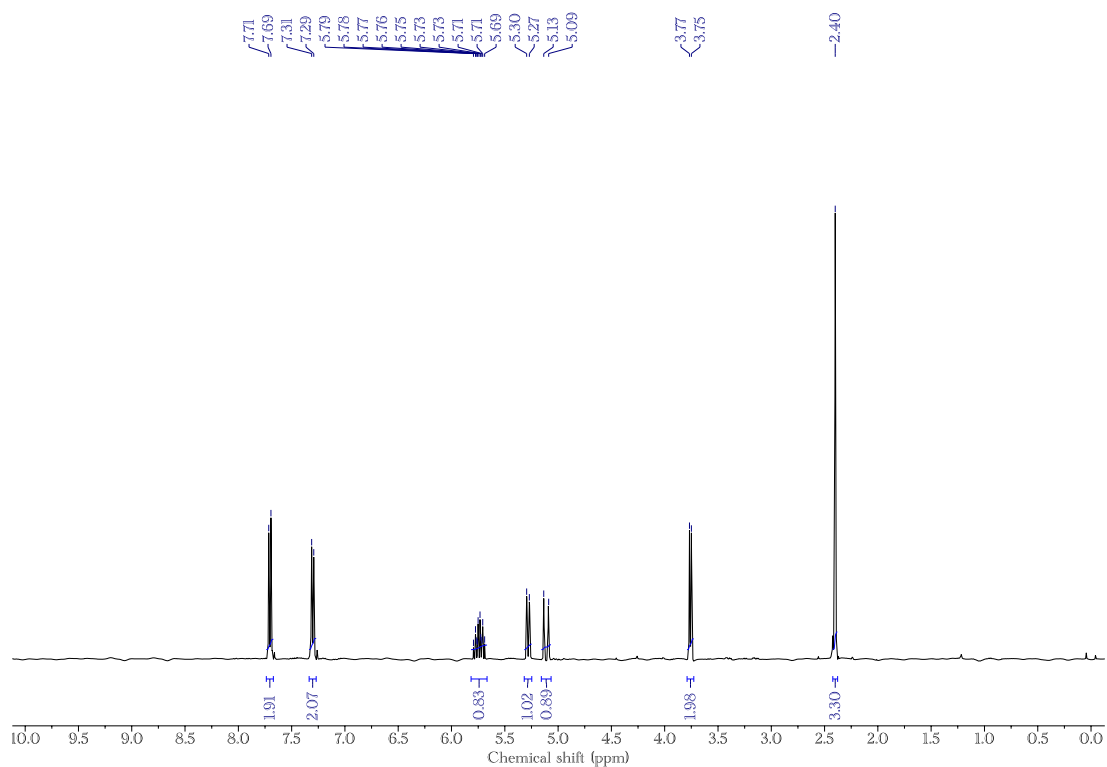
¹³C NMR spectrum (150 MHz, CDCl₃) of compound 3c



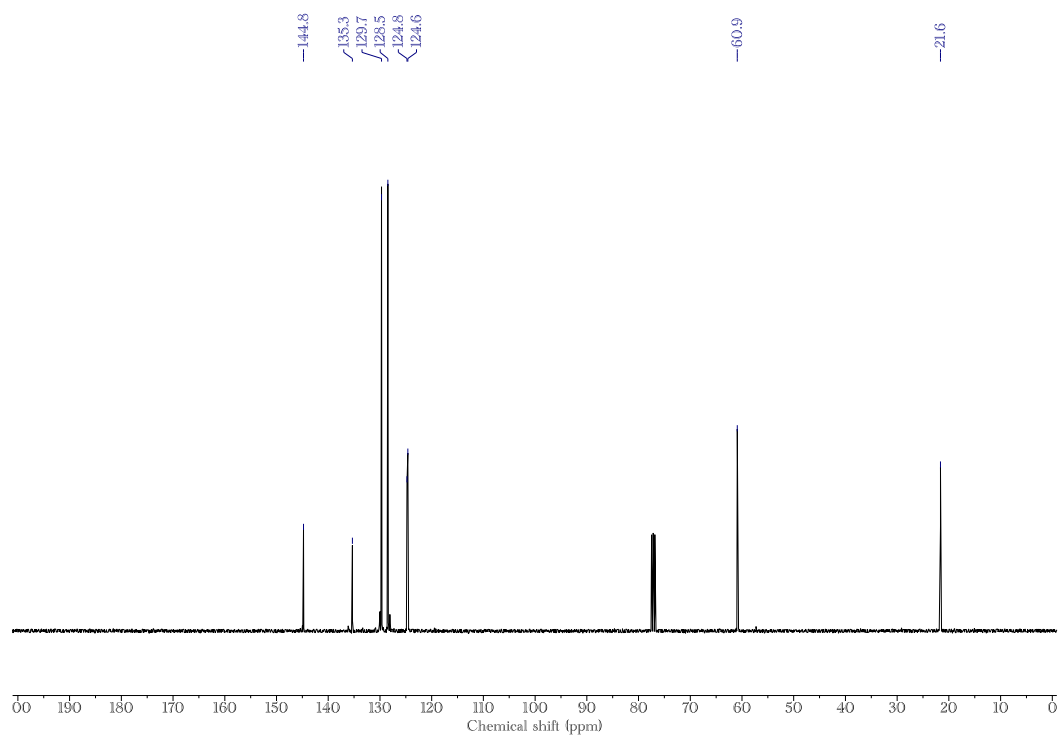
¹H NMR spectrum (400 MHz, CDCl₃) of compound 3d



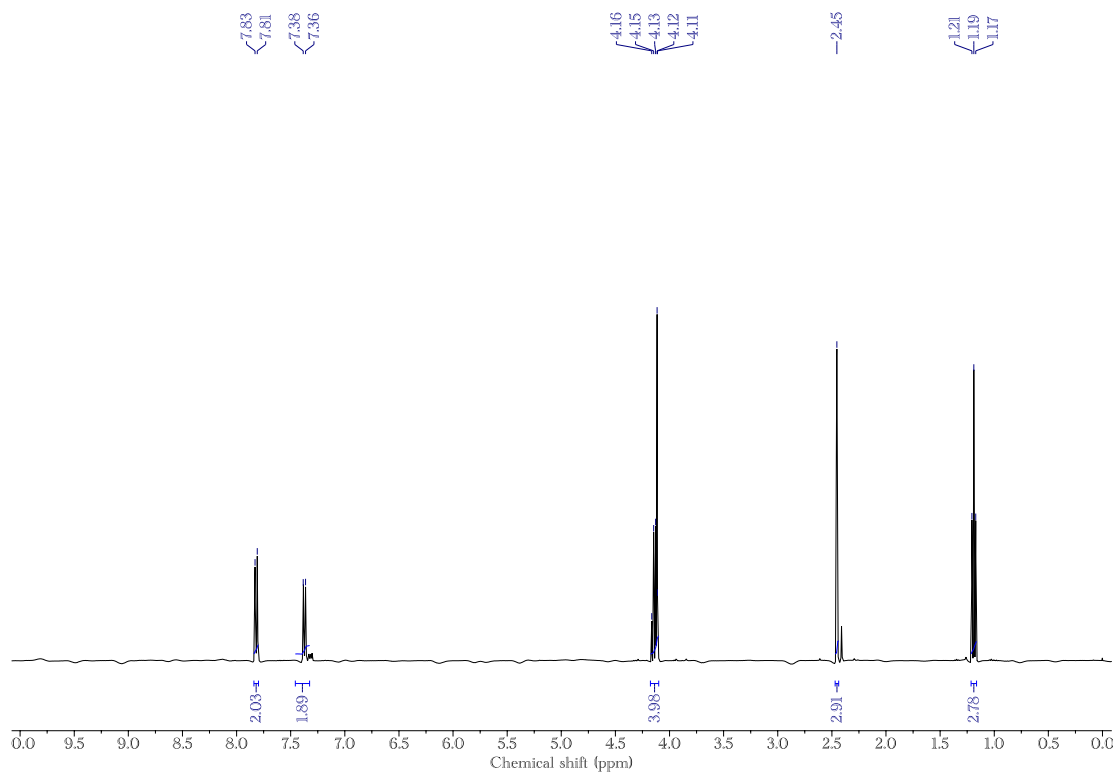
¹³C NMR spectrum (100 MHz, CDCl₃) of compound 3d



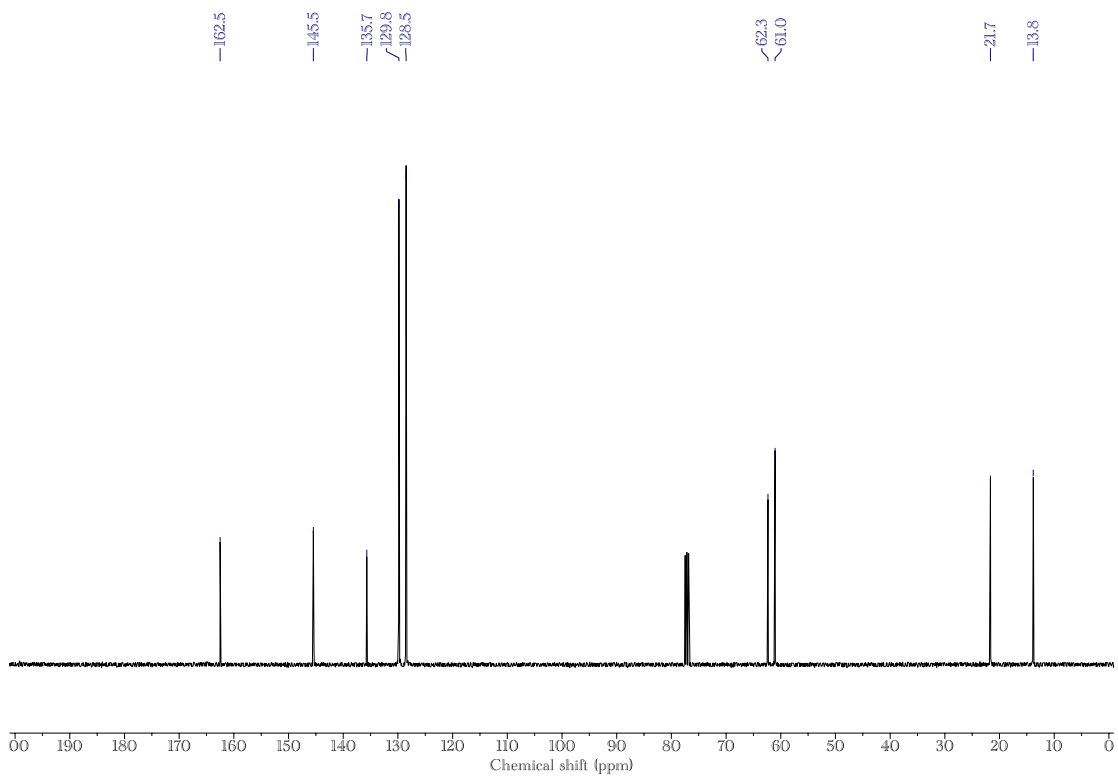
¹H NMR spectrum (400 MHz, CDCl₃) of compound 3e



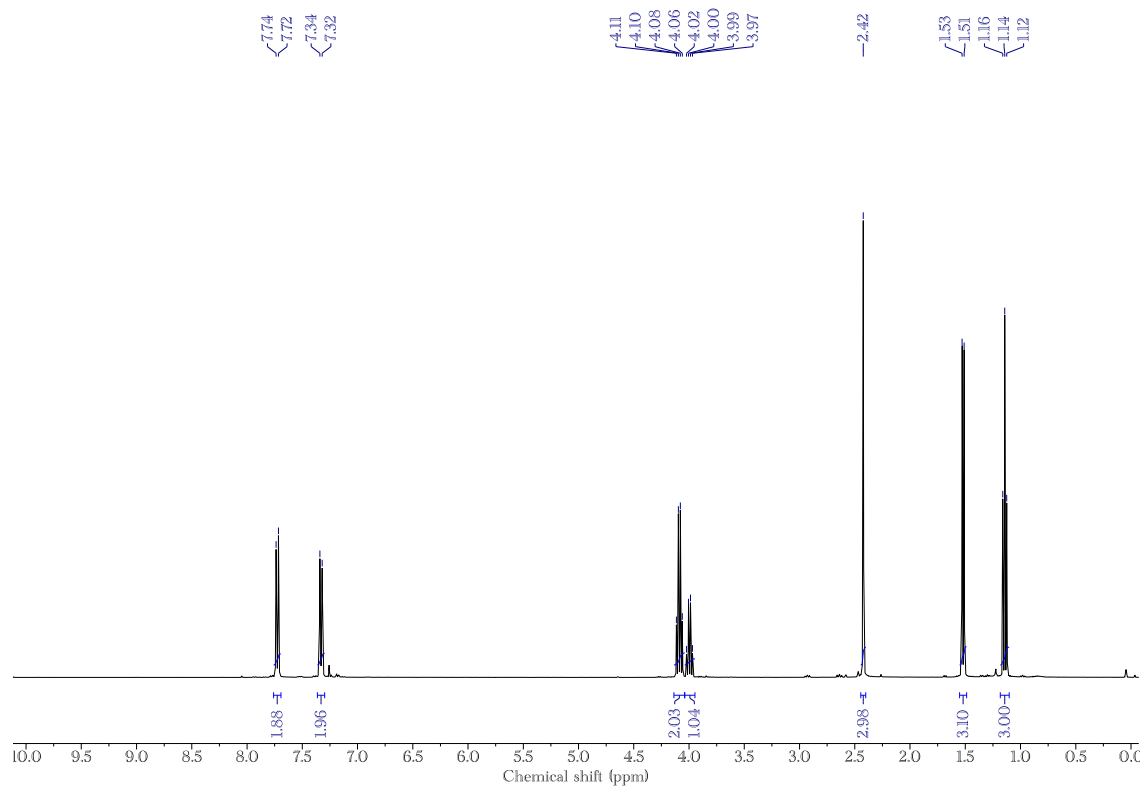
¹³C NMR spectrum (100 MHz, CDCl₃) of compound 3e



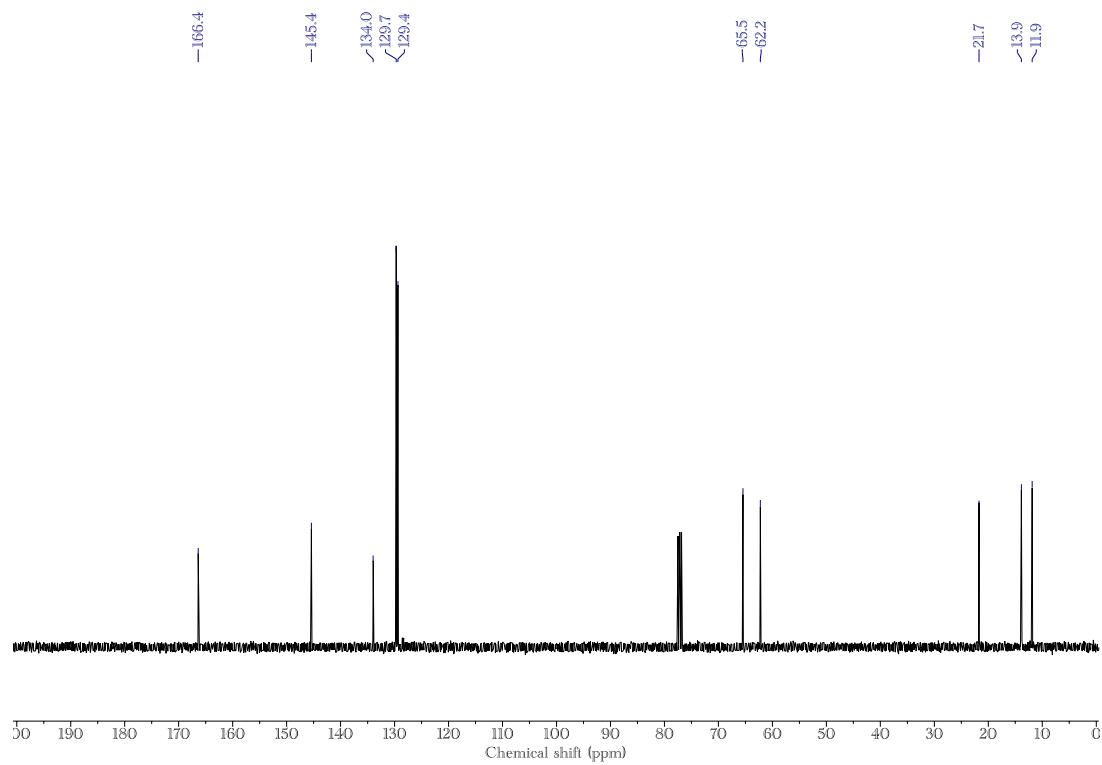
^1H NMR spectrum (400 MHz, CDCl_3) of compound 3f



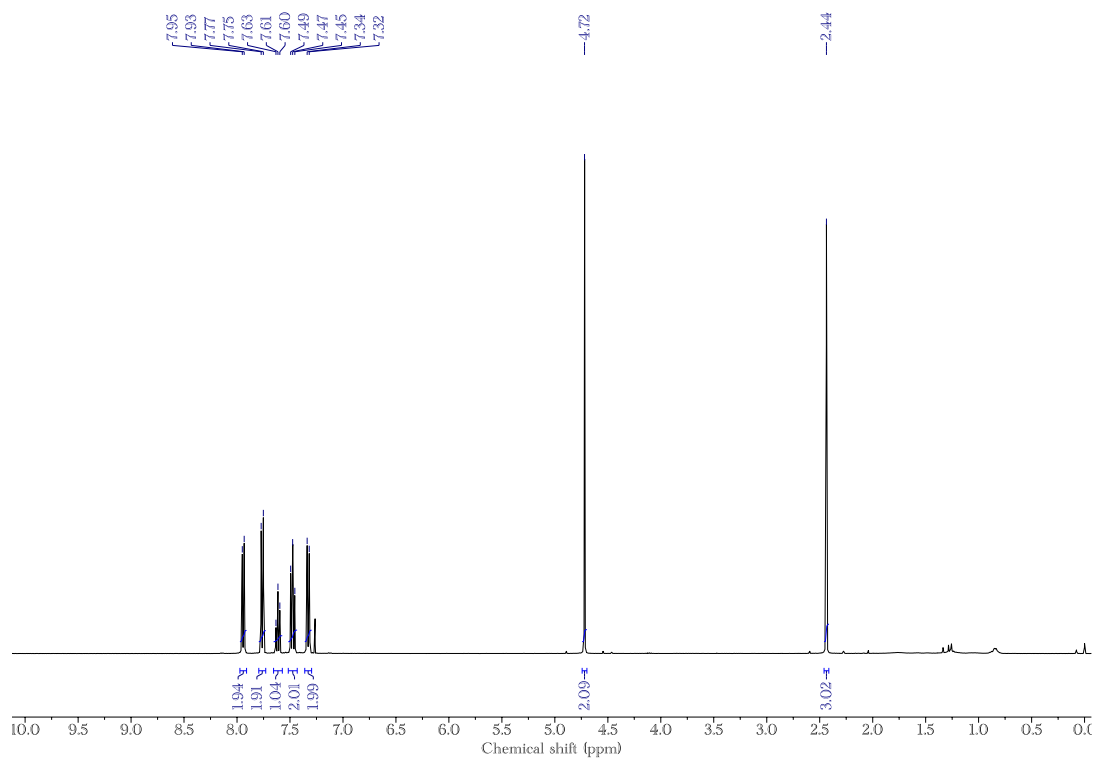
^{13}C NMR spectrum (100 MHz, CDCl_3) of compound 3f



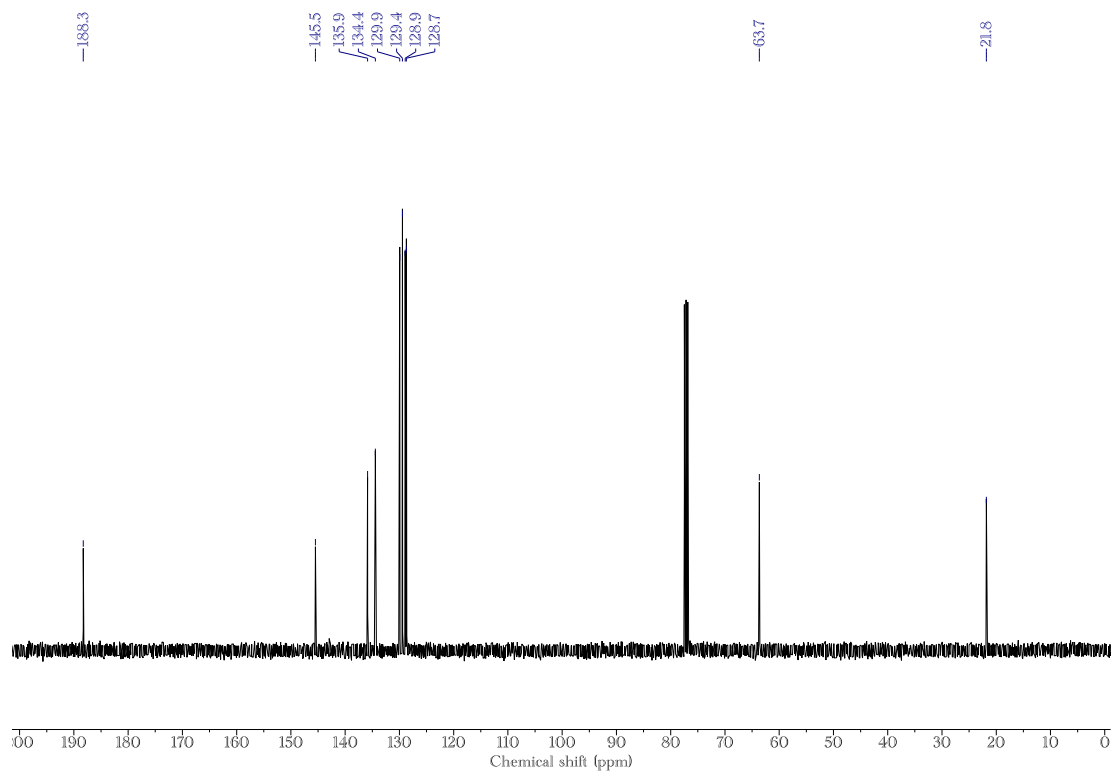
¹H NMR spectrum (400 MHz, CDCl₃) of compound 3g



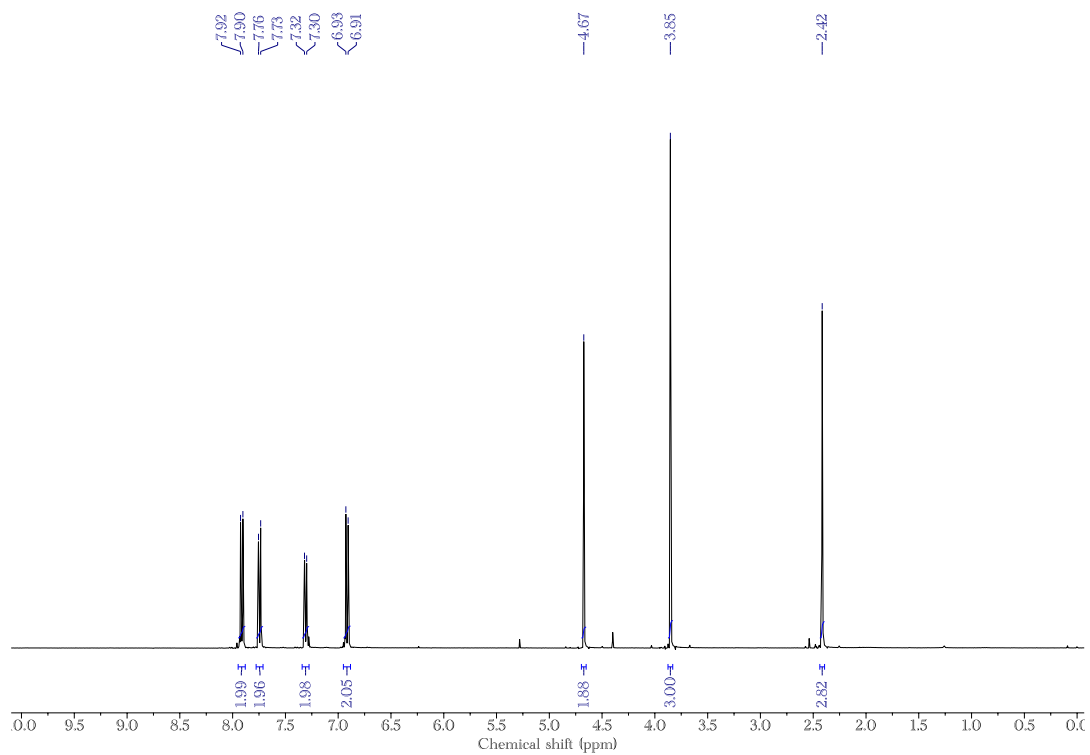
¹³C NMR spectrum (100 MHz, CDCl₃) of compound 3g



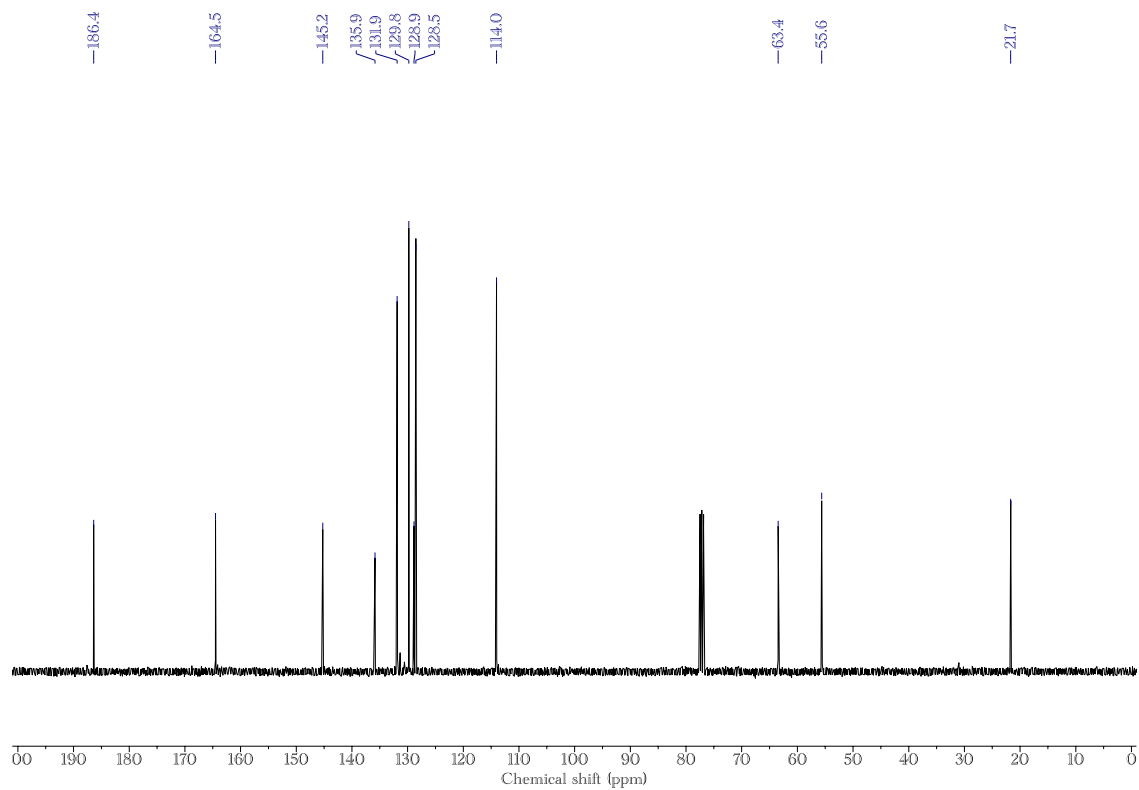
¹H NMR spectrum (400 MHz, CDCl₃) of compound 3k



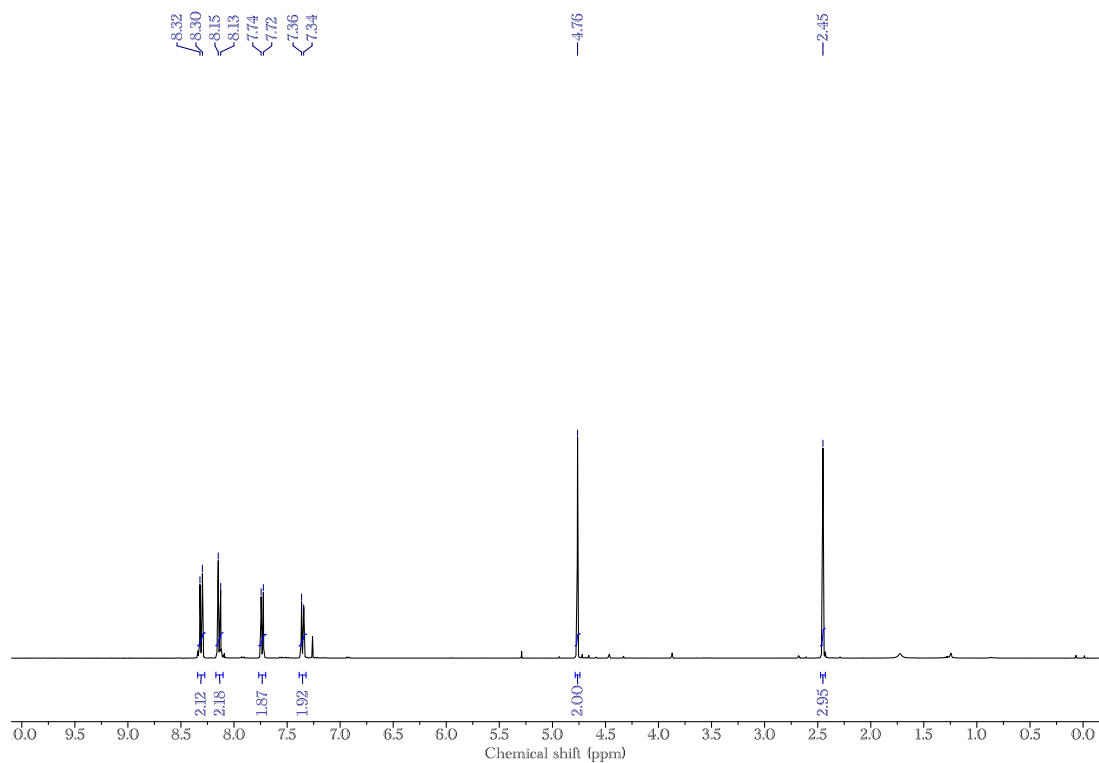
¹³C NMR spectrum (100 MHz, CDCl₃) of compound 3k



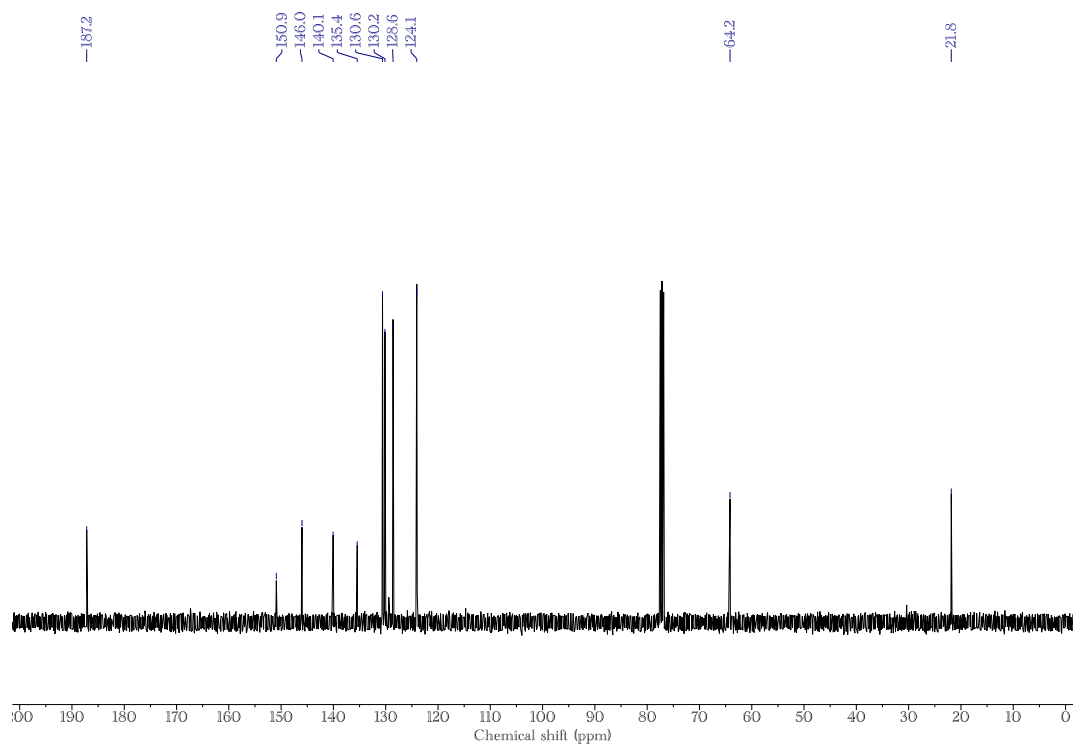
¹H NMR spectrum (400 MHz, CDCl₃) of compound 31



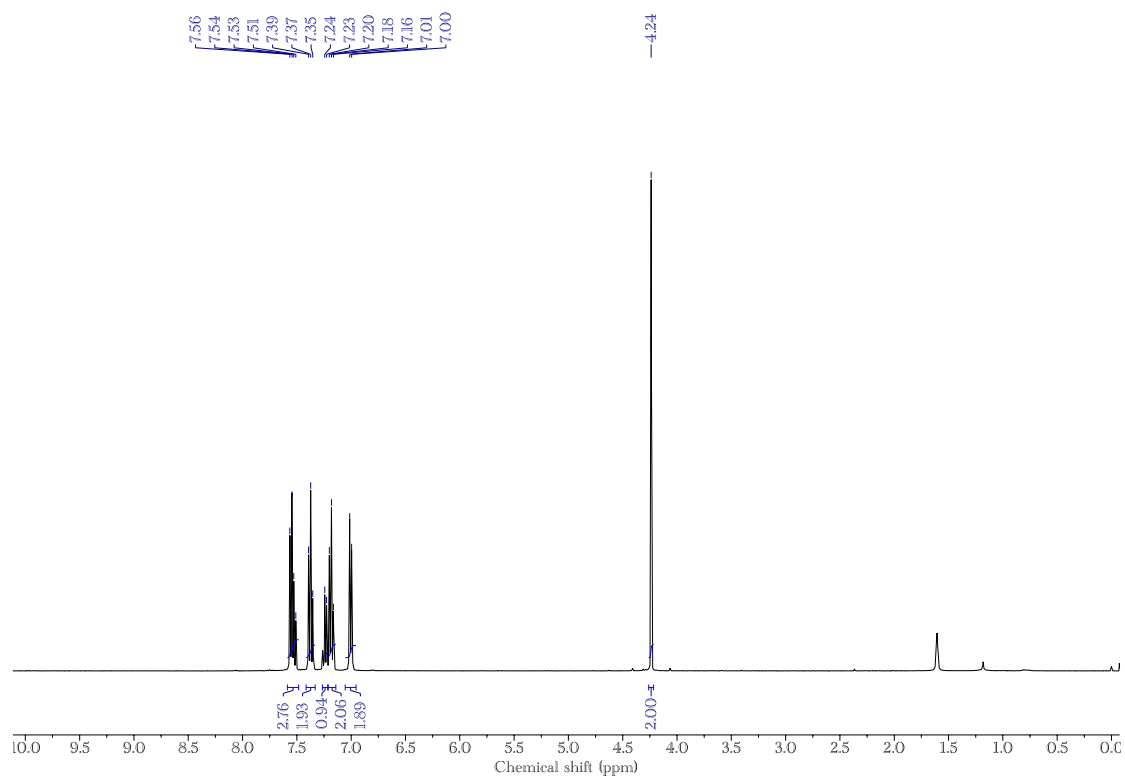
¹³C NMR spectrum (100 MHz, CDCl₃) of compound 31



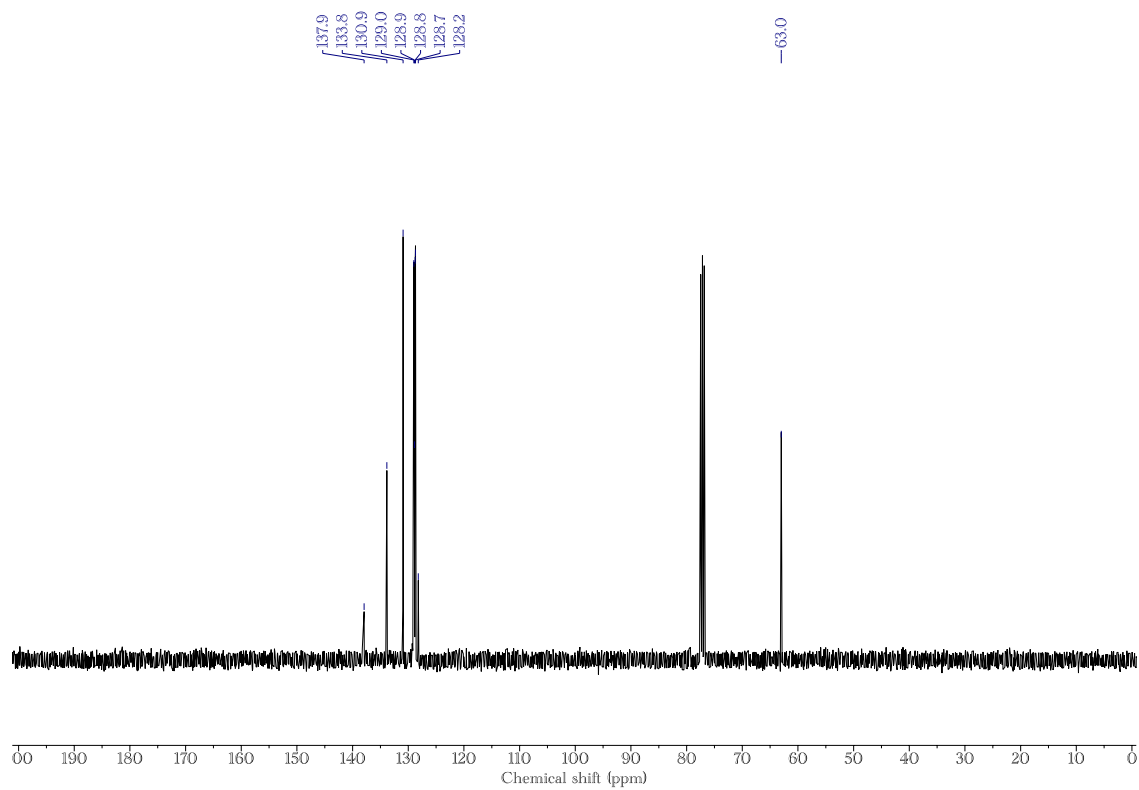
¹H NMR spectrum (400 MHz, CDCl₃) of compound 3m



¹³C NMR spectrum (100 MHz, CDCl₃) of compound 3m



¹H NMR spectrum (400 MHz, CDCl₃) of compound 3n



¹³C NMR spectrum (100 MHz, CDCl₃) of compound 3n

4. EcoScale comparative analysis of sulfonylation procedures described in literature.

Table S3. EcoScale penalty points¹² of sulfonylation reactions described in literature.¹³⁻¹⁷

Entry	Parameters	C(sp ³)-H sulfonylation ¹³	C(8)-H sulfonylation ¹⁴	<i>In situ</i> generation of sulfinate ion ¹⁵	sulfinate /bismuth reagent ¹⁶	sulfinate/BnBr phase transfer catalyst ¹⁷	This work
1	Yield	16.5	14	2	0.5	1	4
2	Price of reaction componentes	5	5	5	5	3	0
3	Safety	30	45	45	35	25	20
4	Technical setup	2	1	0	1	2	2
5	Temperature/time	1	3	3	3	2	1
6	Workup and purification	13	13	13	10	13	3
7	Penalty points total	67.5	81	68	54.5	46	30

5. References

- 1 S. G. B. Passos, D. V. Freitas, J. M. M. Dias, E. T. Neto and M. Navarro, *Electrochim. Acta*, 2016, **190**, 689–694.
- 2 D. V. Freitas, J. R. González-Moya, T. A. S. Soares, R. R. Silva, D. M. Oliveira, H. S. Mansur, G. Machado and M. Navarro, *ACS Appl. Energy Mater.*, 2018, **1**, 3636–3645.
- 3 M. Masteri-Farahani and K. Khademabbasi, *J. Lumin.*, 2018, **204**, 130–134.
- 4 M. Amelia, C. Lincheneau, S. Silvi and A. Credi, *Chem. Soc. Rev.*, 2012, **41**, 5728.
- 5 M. A. Reddy, P. S. Reddy and B. Sreedhar, *Adv. Synth. Catal.*, 2010, **352**, 1861–1869.
- 6 J. Barluenga, M. Tomás-Gamasa, F. Aznar and C. Valdés, *European J. Org. Chem.*, 2011, **2011**, 1520–1526.
- 7 G. C. Tsui and M. Lautens, *Angew. Chemie Int. Ed.*, 2010, **49**, 8938–8941.
- 8 H. Wang, P. Lian, Y. Zheng, J. Li and X. Wan, *Org. Biomol. Chem.*, 2020, **18**, 2163–2169.
- 9 A. S. Kende and J. S. Mendoza, *J. Org. Chem.*, 1990, **55**, 1125–1126.

- 10 N. Kumar and A. Kumar, *ACS Sustain. Chem. Eng.* 2019, **7**, 9182–9188.
- 11 N. Fukuda and T. Ikemoto, *J. Org. Chem.* 2010, **75**, 4629–4631.
- 12 K. V. Aken, L. Strekowski and L. Patiny, *Beilstein J. Org. Chem.* 2006, **2**, 1-7.
- 13 P. J. Sarver, N. B. Bissonnette and D. W. C. MacMillan, *J. Am. Chem. Soc.* 2021, **143**, 9737–9743.
- 14 Y. Sun, C. Feng, P. Wang, F. Yang and Y. Wu, *Org. Chem. Front.* 2021, **8**, 5710–5715.
- 15 P. K. Shyam and H.-Y. Jang, *J. Org. Chem.* 2017, **82**, 1761–1767.
- 16 F. Zhao and X-F. Wu, *Organometallics* 2021, **40**, 2400–2404.
- 17 X.-L. Shi, Y. Chen, Q. Hu, H. Meng, and P. Duan *Ind. Eng. Chem. Res.*, 2018, **57**, 7450-7457.